Preprints of the 21st IFAC World Congress (Virtual)
Berlin, Germany, July 12-17, 2020

# Flow-based Flight Routing and Scheduling under Uncertainty

**Gammana Guruge Nadeesha Sandamali, Rong Su, Kalupahana Liyanage Kushan Sudheera**

*School of Electrical and Electronic Engineering at Nanyang Technological University, Singapore 639798. (e-mail: nadeesha001@e.ntu.edu.sg, rsu@ntu.edu.sg, kushansu001@e.ntu.edu.sg)*

**Abstract:** To tackle the future air traffic demands and to enhance the safety of the Air Transportation System (ATS), a proper flight routing and scheduling scheme is required. This paper proposes an Air Traffic Flow Management (ATFM) model while considering the inherent uncertainties present in the ATS. The proposed model aims to reduce capacity violations and conflicts with the use of a probabilistic approach of chance constraint while minimizing adverse effects due to demand and capacity uncertainties. Further, the proposed approach uses the concept of flow-based modeling in which a set of flights are considered as a flow, to enlarge the problem space with the added feature of scalability. In the end, a flow decomposition strategy is used to obtain the individual flight information from the flow results. To the best of our knowledge, this is the first attempt to propose an ATFM model with a flow-based structure while considering both demand and capacity uncertainties. The optimization problem is formulated as an Integer Linear Programming (ILP) problem. The NP-hard nature of the overall problem is minimized by transforming the problem into a Maximum Weighted Independent Set (MWIS) finding problem.

*Keywords:* Air Traffic Flow Management, Stochastic Programming, Optimization, Scheduling, Uncertainty

## 1. INTRODUCTION

With the growth of demand in air transportation, efficient Air Traffic Flow Management (ATFM) and Air Traffic Control (ATC) services are indeed required for the betterment of the overall Air Transportation System (ATS). Similarly, the importance of safety is crucial to provide a reliable and trustworthy air transportation service. With this motivation, our intention of this paper is to propose an ATFM model that can be expanded over large scale networks with the consideration of inherent uncertainty in the system.

In this paper, we consider two main types of uncertainties present in the ATS, which are demand uncertainty and capacity uncertainty, Smith and Gilbo (2005). The root causes for the demand uncertainty are the departure time deviation and cruising speed deviation, which eventually develops unexpected flow deviations. The unpredictable variation in weather conditions and controller workload are the two major factors for the uncertainty of capacity. From the existing literature on ATFM, Bertsimas et al. (2011), Wei et al. (2013), Zhang et al. (2018), and Bertsimas and Patterson (1998) have considered solving large scale en-route ATFM problems. However, these models lack consideration of the above described uncertainty types, thus, less applicable in uncertain situations.

Only a few studies have incorporated the inherent uncertainty in ATFM. Among them, Balakrishnan and Chandran (2014), Clarke et al. (2009), Chen et al. (2017) have considered only capacity uncertainty, while Sandamali et al. (2020), Sandamali et al. (2017) have considered only demand uncertainty in flight scheduling yet at a flight-by-flight level. Most of the existing work has used the concept of scenario tree approach, Balakrishnan and Chandran (2014), Clarke et al. (2009) to take into the consideration of uncertainty. However, the scenario tree-based stochastic modeling approach has the main limitation of complexity in expanding over large scale scenario sets. To overcome such formulation difficulties, here, we use a probabilistic approach of chance constraint in our model to guarantee that the stochastic constraints are satisfied with a certain level of confidence. However, none of the above mentioned literature has considered both demand and capacity and their imbalance in flight routing and scheduling.

In contrast, we have proposed an ATFM model in our previous work Sandamali et al. (Under review) using a flight-by-flight structure, while scrutinizing both uncertainties types. But, it has a major drawback in terms of the associated computational complexity due to the involvement of a very large number of decision variables with a flight-by-flight formulation structure. Thus, here, we use the concept of flow, which is defined as a group of flights, to reduce the computational difficulties in our previous work. Among the existing flow-based model, Zhang et al. (2018), Sun and Bayen (2008), and Cao and Sun (2011) have used the basic concept of cell transmission to describe the flow dynamics in detail.

With regards to the solution strategy, we use a Maximum Independent Set (MIS) based approach to reduce the

computational complexity of our model, by decomposing the problem into a set of independent sub-flows.

The contributions of this paper are listed below.

(1) An ATFM model, which takes en-route capacity uncertainty and demand uncertainty (in terms of flow uncertainty) into account, while enhancing the scalability.
(2) Minimization of violations and conflicts due to uncertainties present in the system, thus enhancing the safety of the ATS.
(3) An efficient solution mechanism, which can be applied in solving realistic large scale ATFM problems.

The remainder of the paper is structured as follows. Section 2 describes the problem statement and the ATFM system. Section 3 depicts the proposed flow-based ATFM model in detail and the solution mechanism. The experimental results are illustrated in section 4, and finally, section 5 concludes the paper.

## 2. PROBLEM STATEMENT AND ATFM SYSTEM

### *2.1 Problem Statement*

Inherent uncertainties in ATS can induce unforeseen situations such as unexpected demand in air routes/sectors, flight delays, higher workload for ATCs, safety risks, etc... When the flights deviate from the scheduled time, there are possibilities for unexpected demand in some sectors/links. Similarly, the en-route speed can also be deviated from the nominal values due to wind uncertainty, engine efficiency, pilot behavior, etc.. Sandamali et al. (2019).Thus, the two main factors for the time deviation can be identified as departure delays and speed deviations, which eventually result in flow uncertainties. With the increase in traffic demand, this can be devastated. Thus, it is important to consider the demand uncertainty in ATFM. Moreover, the sector capacity is also an uncertain factor, mainly due to weather fluctuation, emergency situations, etc... This can even cause a higher controller workload, congestion, and safety risks. Depending on the air traffic controller's efficiencies, the handling capacities can vary as shown in it. Thus, we aim in this work to take both demand and capacity uncertainties into consideration in flight routing and scheduling to minimize the controller workload, conflicts/violations, and to enhance the safety of the overall ATS.

### *2.2 ATFM System*

*Structure of the air traffic network (ATN):-* The ATN is a graph of connected waypoints ($w \in W$) via air routes/links ($j \in J$) with capacitated elements of airports, links, and sectors. Each airport consists of a departure link ($d$) and an arrival link ($a$). Waypoints are a two-dimensional location of the airspace, which are used for radar navigation. Links are the direct connection between two waypoints with length denoted as $L_j$. The set of flights is denoted as $F$ with, $f_k \in F$. Each flow is differentiated by the OD pair $o \in O_p$ and aircraft type $\lambda \in \phi$. The notations used in our model are listed below.

- $\underline{V}^{\lambda}, \bar{V}^{\lambda}$ - Maximum and minimum crusing speed of aircraft type $\lambda$.
- $T_{min}, L_{min}$ - Required minimum in-trail time and distance separation, separately.
- $T_{PH}, t_{\triangle}$ - Prediction horizon and the duration of a discrete time slot, respectively. $t$ denotes the time index, which is an integer such that $t \in T$, where $T$ is the total number of sampling points in the prediction horizon and $T_{PH} = t_{\triangle} * T$.
- $F_j^{o,\lambda}(t), \tilde{F}_j^{o,\lambda}(t)$ - Deterministic and stochastic flows with OD pair $o$ and type $\lambda$ in route $j$ at time interval $t$, respectively. $j \rightarrow w$ for waypoint.
- $\triangle_{F_j}(t)$ - Uncertainty of flow (deviation from the deterministic value) in route $j$ at time interval $t$.
- $F_{j,in}^{o,\lambda}(t), F_{j,out}^{o,\lambda}(t)$ - The number of incoming and outgoing flights with OD pair $o$ and type $\lambda$ in route $j$ at time $t$. $j \rightarrow d$ for the departure link and $j \rightarrow a$ for the arrival link, $d \in J_D, a \in J_A$ where $J_D$ and $J_A$ are the set of all departure and arrival links.
- $F_{j,j'}^{o,\lambda}(t)$ - The number of aircraft entering from link $j$ to $j'$ with OD pair $o$ and type $\lambda$ at time $t$.
- $\triangle_w^{f_i}$ - Arrival time uncertainty of $f_i$ at waypoint $w$.
- $\tilde{V}_s(t), \tilde{C}_s(t)$ - Stochastic volume and capacity of sector $s$ at time $t$.
- $J_j^o(U), J_j^o(D)$ - Set of upstream and downstream links connected with link $j$ for the OD pair $o$, respectively. $j \rightarrow w$ for waypoint.

## 3. FLOW BASED ATFM MODEL FORMULATIONS

### *3.1 Flow dynamic constraints*

The constraints in (1) describe the relationship of link volume with its adjacent link flows i.e., with incoming and outgoing flows. $(\forall t \in T)(o \in O_p)(\lambda \in \phi)$

$$(\forall j \in J - J_A) F_{j,in}^{o,\lambda}(t) = \sum_{j'' \in J_j^o(U)} F_{j'',j}^{o,\lambda}(t) \tag{1a}$$

$$(\forall j \in J - J_a^o(U)) F_{j,out}^{o,\lambda}(t) = \sum_{j' \in J_j^o(D)} F_{j,j'}^{o,\lambda}(t) \tag{1b}$$

Then, the flow at time $t + \triangle t$ can be derived as,

$$F_j^{o,\lambda}(t + \triangle t) = F_j^{o,\lambda}(t) + \left[ F_{j,in}^{o,\lambda}(t) - F_{j,out}^{o,\lambda}(t) \right] \tag{1c}$$

### *3.2 Link capacity constraint*

This constraint is used to limit the link volume based on the link length and the head-tail distance separation between flights.

$$(\forall t \in T)(\forall j \in J) \quad \sum_{o \in O_p, \lambda \in \phi} \tilde{F}_j^{o,\lambda}(t) \leq \frac{L_j}{L_{min}} \tag{2a}$$

Let's take, $\tilde{F}_j(t) = \sum_{o \in O_p, \lambda \in \phi} \tilde{F}_j^{o,\lambda}(t)$. Since the link volume can deviate from the scheduled value due to uncertainty of demand, the distribution of $\tilde{F}_j(t)$ is obtained based on the historical data of flights' actual link arrival and exit times and approximated by a normal distribution such that, $\tilde{F}_j(t) \sim N(\mu_{\tilde{F}_j}(t), \sigma_{\tilde{F}_j}(t))$. By applying chance constraint to ensure that the constraint in (2a) will be satisfied with a probability of $\beta$.

$$P(\tilde{F}_j(t) \leq C_j) \geq \beta \tag{2b}$$

Where, $C_j = \frac{L_j}{L_{min}}$. The above constraint can be re-written using deterministic and uncertain components of $\tilde{F}_j(t)$ as,

$$P(F_j(t) + \triangle_{F_j}(t) \leq C_j) \geq \beta \tag{2c}$$

Converting into a linear constraint using cumulative distribution function (CDF),

$$F_{\triangle_{F_j}(t)}(C_j - F_j(t)) \geq \beta \tag{2d}$$

$$C_j - F_j(t) \geq \zeta_{\triangle_{F_j}(t)} \tag{2e}$$

Where, $\zeta_{\triangle_{F_j}(t)}$ represents the inverse of $F_{\triangle_{F_j}(t)}$. The CDF of a normal distribution can be written as in (2f) (For $\zeta_{\triangle_{F_j}(t)} \geq \mu_{\triangle_{F_j}}(t)$) Linhart (2008).

$$\frac{1}{2}\left(1 + erf(\frac{\zeta_{\triangle_{F_j}(t)} - \mu_{\triangle_{F_j}}(t)}{\sqrt{2}\sigma_{\triangle_{F_j}}(t)})\right) \geq \beta \tag{2f}$$

Thus, the linear interpretation of (2e) can be derived as,

$$F_j(t) \leq C_j - \mu_{\triangle_{F_j}}(t) - \sqrt{2}\sigma_{\triangle_{F_j}}(t) erf^{-1}(2\beta - 1) \tag{2g}$$

*Note: The distribution of the link flow uncertainty can be obtained based on the distribution of $\tilde{F}_j(t)$ and $F_j(t)$, which can be obtained using flights' scheduled link arrival and exit times. Hence, $\triangle_{F_j}(t) \sim N(\mu_{\triangle_{F_j}}(t), \sigma_{\triangle_{F_j}}(t))$ with $\mu_{\triangle_{F_j}}(t) = \mu_{\tilde{F}_j}(t) - F_j(t)$ and $\sigma_{\triangle_{F_j}}(t) = \sigma_{\tilde{F}_j}(t)$.*

### *3.3 Sector capacity constraint*

We use this constraint to limit the sector volume by the sector capacity under uncertain conditions as in (3a).

$$\tilde{V}_s(t) \leq \tilde{C}_s(t) \tag{3a}$$

Applying a chance constraint probability of $\beta_S$ into (3a),

$$P(\tilde{V}_s(t) \leq \tilde{C}_s(t)) \geq \beta_S \tag{3b}$$

By separating deterministic and uncertain components,

$$P(V_s(t) + \triangle_{V_s}(t) \leq C_s(t) + \triangle_{C_s}(t)) \geq \beta_S \tag{3c}$$

Let, $\triangle_{V_s,C_s}(t) = \triangle_{V_s}(t) - \triangle_{C_s}(t)$

$$P(\triangle_{V_s,C_s}(t) \leq C_s(t) - V_s(t)) \geq \beta_S \tag{3d}$$

Applying similar steps in (2d)-(2g), the linear interpretation of (3d) can be derived as follows.

$$V_s(t) \leq C_s(t) - \mu_{\triangle_{V_s,C_s}}(t) - \sqrt{2}\sigma_{\triangle_{V_s,C_s}}(t) erf^{-1}(2\beta_S - 1) \tag{3e}$$

*Note: The distribution of the sector volume uncertainty distribution ($\triangle_{V_s}(t)$) can be obtained using previous flight records of sector entry, exit times and approximated by a normal distribution such that, $\triangle_{V_s}(t) \sim N(\mu_{\triangle_{V_s}}(t), \sigma_{\triangle_{V_s}}(t))$. Based on the historical sector capacity data, the best fitted normal distribution of $\triangle_{C_s}(t)$ is obtained with mean and standard deviation of $\mu_{\triangle_{C_s}}(t)$ and $\sigma_{\triangle_{C_s}}(t)$. Then, the distribution of $\triangle_{V_s,C_s}(t)$ is derived with mean and standard deviation of $\mu_{\triangle_{V_s,C_s}}(t) = \mu_{\triangle_{V_s}}(t) - \mu_{\triangle_{C_s}}(t)$ and $\sigma_{\triangle_{V_s,C_s}}(t) = \sqrt{\sigma_{\triangle_{V_s}}(t)^2 + \sigma_{\triangle_{C_s}}(t)^2}$.*

### *3.4 Waypoint flow rate constraint*

We use this constraint to limit the merging flow at waypoints is to be lower than its capacity, which is determined by the discrete time slot size and the head-tail time separation. The flow at a waypoint ($F_w(t)$) is the summation of flows traversing from upstream links to downstream links through the waypoint.

$$(\forall t \in T) \;\; F_w(t) = \sum_{j'' \in J_w^o(U), j \in J_w^o(D), o \in O_p, \lambda \in \phi} F_{j'',j}^{o,\lambda}(t) \tag{4a}$$

By constraining with the waypoint capacity,

$$(\forall t \in T)(\forall w \in W) \;\; \tilde{F}_w(t) \leq \frac{t_\triangle}{T_{min}} \tag{4b}$$

Applying a chance constraint with a probability of $\beta_W$,

$$P(\tilde{F}_w(t) \leq \frac{t_\triangle}{T_{min}}) \geq \beta_W \tag{5}$$

$$P(\triangle_{F_w}(t) \leq t_\triangle/T_{min} - F_w(t)) \geq \beta_W \tag{6}$$

Applying similar steps in (2d)-(2g), the linear representation of (6) can be derived as follows.

$$F_w(t) \leq t_\triangle/T_{min} - \mu_{\triangle_{F_w}}(t) - \sqrt{2}\sigma_{\triangle_{F_w}}(t) erf^{-1}(2\beta_W - 1) \tag{7}$$

*Note: The distribution of $\triangle_{F_w}(t)$ is obtained using previous records of waypoint arrival time and obtain the values for $\mu_{\triangle_{F_w}}(t)$ and $\sigma_{\triangle_{F_w}}(t)$.*

### *3.5 Flow shift constraint*

Flow shift constraint is used to bound the link traversing time between their lower and upper bounds, which depends on link length and minimum and maximum cruise speed. To divide the range into discrete slots, the ceiling and floor functions are used as follows.

$$\left\lceil \frac{L_j}{\bar{V}^\lambda * t_\triangle} \right\rceil \leq T_n^\lambda(j) \leq \left\lfloor \frac{L_j}{\underline{V}^\lambda * t_\triangle} \right\rfloor \tag{8a}$$

where $\lceil . \rceil$ and $\lfloor . \rfloor$ denotes ceiling and floor functions, respectively. $T_n^\lambda(j)$ is an integer representing total traversing time in discrete points.

When there are short links, the above constraint is applied for the aggregated links. For long links, they partition into several links in such a way that there is an unique shift of time such that, $\underline{T}_n^\lambda(j) = \bar{T}_n^\lambda(j)$. (let's take it as $n(j)$). This will also ensure that the first entered flow will leave the link first without allowing flow overtake situations.

Further, the constraint in (8b) ensures that the incoming flow to a link should exit the link in a subsequent time step. Moreover, the outgoing flow of the link at $t$ should not be higher than the volume of the link at $t$ as in (8c).

$$F_{i,in}^{o,\lambda}(t) = F_{i,out}^{o,\lambda}(t + n(j)) \tag{8b}$$

$$F_{i,out}^{o,\lambda}(t) \leq F_i^{o,\lambda}(t) \tag{8c}$$

### *3.6 Flow upper bounds*

The constraints in (9a) and (9b) set the upper bounds for the departure and arrival rates, respectively, in such a way that they will not exceed the scheduled flow rates.

$$(o \in O_p)(\lambda \in \phi) \sum_{t \in T} F_{d,out}^{o,\lambda}(t) \leq \sum_{t \in T} \gamma_{d,out}^{o,\lambda}(t) \tag{9a}$$

$$(o \in O_p)(\lambda \in \phi) \sum_{t \in T} F_{a,in}^{o,\lambda}(t) \leq \sum_{t \in T} \gamma_{a,in}^{o,\lambda}(t) \tag{9b}$$

Where, $\gamma^{o,\lambda}_{d,out}(t)$ and $\gamma^{o,\lambda}_{a,in}(t)$ denote the scheduled departure and arrival flow rates, respectively.

### *3.7 Objective Function*

Our main objective is to dispatch and receive all flows in their respective time slots. The first term is to penalize the departure flow deviation, while the second term is to penalize the arrival flow deviation. According to (10), flows will always try to dispatch/arrive at their scheduled time slots or more closer to them, since the deviation adds higher penalties to the objective function. The coefficients are gradually decreased with the deviation of the flow from the scheduled time. $\underline{t}^{o,\lambda}_d, \bar{t}^{o,\lambda}_d$ are the minimum and maximum allowable departure time limits and $\underline{t}^{o,\lambda}_a, \bar{t}^{o,\lambda}_a$ are the respective values for the arrival time limits. $M_d$ and $M_a$ are two big constants. The third term forces the total flight flow to be scheduled without incurring any cancellations.

$$min \sum_{d\in J_D, o\in O_p, \lambda\in\phi} \Bigg\{ \sum_{\tilde{t}\in T_d, t\in t_d} C_D(M_d - c_d(\tilde{t}-t)^2)[\gamma^{o,\lambda}_{d,out}(\tilde{t}) - F^{o,\lambda}_{d,out}(t)] + \sum_{\tilde{t}\in T_a, t\in t_a} C_A(M_a - c_a(\tilde{t}-t)^2)[\gamma^{o,\lambda}_{a,in}(\tilde{t}) - F^{o,\lambda}_{a,in}(t)] \Bigg\} - \sum_{a\in J_A, o\in O_p, \lambda\in\phi} C^{o,\lambda}_C \Bigg( \sum_{t\in t_a} F^{o,\lambda}_{a,in}(t) - \sum_{t\in t_a} \gamma^{o,\lambda}_{a,in}(t) \Bigg) \tag{10}$$

where $T_d = \{\tilde{t} \in T | \gamma^{o,\lambda}_{d,out}(\tilde{t}) > 0\}$ , $T_a = \{\tilde{t} \in T | \gamma^{o,\lambda}_{a,in}(\tilde{t}) > 0\}$ and $t_d = \{\tilde{t} - \underline{t}^{o,\lambda}_d : \tilde{t} + \bar{t}^{o,\lambda}_d\}$ , $t_a = \{\tilde{t} - \underline{t}^{o,\lambda}_a : \tilde{t} + \bar{t}^{o,\lambda}_a\}$.

$C_D$, $C_A$ and $C^{o,\lambda}_C$ denote the departure, arrival flow rate coefficients and flow cancellation coefficient, respectively.

The above formulated integer linear programming (ILP) problem can be summarized as,

*min (10) , subject to (1), (2g), (3e), (4a), (7), (8), (9).*

By solving the above optimization problem, the results of flow values are obtained. In the next topic, we will describe how we transformed them into flights.

### *3.8 Decomposition of flows into flights*

The flow results obtained by solving the above optimization problem are decomposed into individual flights Sudheera et al. (2019), as described in Algorithm 1. The flow decomposition process starts from departure and moves through the intermediate links and finally ends at the arrival. First, the flows at the departure links are assigned incrementally to the corresponding flights, if there are no any canceled flights. In cases where the actual departing flow is less than the expected outgoing flow, then we have to cancel a set of flights. Since there are a set of scenarios to select which flights are canceled, here, we explore all of such scenarios and select the one with the minimum expected flight delay. Then, the remaining flights are assigned incrementally to the departure link at their corresponding times.

Then, the flights are traced at the intermediate links assigning respective air routes and time values based on the flow dynamics and link shift constraints.

**Algorithm 1** Flow decomposition into flights

**Inputs:** $F^{o,\lambda}_{d,out}(t), \gamma^{o,\lambda}_{d,out}(t)$ for all $t, j, o, \lambda, d$

**for each** $p \in (o, \lambda)$ **do**
  $f^p_{act} \leftarrow \sum_{\forall t} F^{o,\lambda}_{d,out}(t)$ ▷ $f^p_{act}$- `total departed flights`
  $f^p_{sch} \leftarrow \sum_{\forall t} \gamma^{o,\lambda}_{d,out}(t)$ ▷ $f^p_{act}$- `total scheduled flights`
  $n^p_c \leftarrow f^p_{sch} - f^p_{act}$ ▷ $n^p_c$ - `number of canceled flights`
  $S^p \leftarrow getAllPermutations(n^p_c, f^p_{sch})$ ▷ $S^p$ - `collection of sets of all flight profiles excluding cancellations`
  PermDelay $\leftarrow []$
  **for each** $s \in S^p$ **do**
    $T_{delay} \leftarrow 0$ ▷ $T_{delay}$- `Total delay`
    **for** $t \in T$ **do** ▷ $t$ - `discrete time steps`
      - Assign $f_k \in s$ departure slot to $t$ unless $f_k$ is already assigned or sum of $f_k$'s at $t$ has already reached $F^p_{d,out}(t)$
      $t^{f_k}_{delay} \leftarrow |\hat{t}^{f_k} - t|$ ▷ `scheduled departure time slot of` $f_k$
      $T_{delay} \leftarrow T_{delay} + t^{f_k}_{delay}$ ▷ `calculate total delay for all` $f_k \in s$
    PermDelay $\leftarrow$ [PermDelay $T_{delay}$]
  $pm_{min} \leftarrow selectPermutation(PermDelay)$ ▷ `Select the permutation with the least total delay`
  **for** $t \in T$ **do**
    - Schedule $f_k \in pm_{min}$ at $t$ unless $f_k$ is already assigned or sum of flights at $t$ has already reached $F^p_{d,out}(t)$
    $Y^{f_k}_d \leftarrow 1$ ▷ `fix departure link`
    $t_0 + (t-1)t_\triangle - \frac{t_\triangle}{2} \leq t^{f_k}_{w'} \leq t_0 + (t-1)t_\triangle + \frac{t_\triangle}{2}$ ▷ $t_0$ - `time offset to match with the initial time slot`, $w'$ - `departure fix`, $t_\triangle$ - `length of a discrete time slot`
At intermediate stages, the flight trajectory (path and time) is traced based on the flow dynamic constraints and link shift constraints.

### *3.9 Solution mechanism : Greedy strategy with maximum weighted independent sets (MWIS)*

Here, we decompose the overall problem into a set of sub-problems based on the flow dependency to minimize the computational complexity. The generated sub-problems are solved iteratively as described in Algorithm 2 below.

**Algorithm 2** Greedy strategy with MWIS

**Step 1:** Convert the Air Traffic Network into a graph, $G = (V, E)$. ▷ $V$ - Time spanned sub-flows, $E$ - Space-time dependency.
Sub-flows are weighted depending on the departure time priority.

**Step 2:** Search and obtain all MISs from the graph. Flow pairs are considered as dependent if any of their trajectories are overlapped in terms of time. Let $S_1, S_2, ..S_n$ denote the independent sets.

**Step 3:** Initialize set, Fixed $= \{\}$. ▷ Empty set, as none of the flows are routed yet

**Step 4: while** (Fixed $\neq$ $V$) ▷ From $S_1$ to $S_n$
1: Schedule $S_i$ on the network with **Fixed** sub-flow set
2: As all sub-flows in an independent set, $S_i$, are conflict free, the solution time is minimal.
3: Fixed $\leftarrow$ (Fixed $\cup$ $S_i$) ▷ Accumulate fixed flows

**Step 5: Fixed** set contains all the routed and scheduled sub flows.

## 4. EXPERIMENTAL RESULTS

We use two case studies consisting of an example grid network and the actual ASEAN air traffic network to evaluate the performance and the real-time applicability of our model. We use MATLAB as the software platform with Gurobi solver (Gurobi (2015)) on a PC with an Intel Core (TM) i5-8250U @1.80GHz CPU and an 8GB of RAM.

### *4.1 Case Study I - Grid network*

In this case study, we used a grid network as shown in Fig. 1, to test the features of our model and to validate it. The network consists of 92 air routes, 8 departure airports, 8 arrival airports, 44 waypoints, and 4 sectors with each having 15 links. We considered 24 OD pairs with 3 flights from each, thus, a total of 72 flights with a time horizon of 10 hours. The discrete time interval is taken as 10 min. To congest the network, the scheduled departure and arrival flows are tightly set. Regarding the uncertainty parameters, the stochastic link flow is taken as, $\tilde{F}_j(t) \sim N(6, 1.3)$ and the uncertain component of the sector volume is taken as $\triangle_{V_s}(t) \sim N(0, 4.6)$. The uncertainty of sector capacity is taken as, $\triangle_{C_s}(t) \sim N(0, 1.0)$, and then, the distribution of $\triangle_{V_s,C_s}(t)$ is estimated as, $\triangle_{V_s,C_s}(t) \sim N(0, 4.7)$. The deterministic sector capacity is set to be 12. Further, the waypoint flow rate uncertainty is taken as, $\triangle_{F_w}(t) \sim N(0, 0.3)$.

*En-route violations with respect to the chance constraint probability:-* In this experiment, our intention is to validate the model in terms of the sector capacity violations and waypoint merging conflict violations with respect to the chance constraint probability. The sector capacity violations are represented as the sum of violations in all four sectors. The merging conflicts are calculated as the number of flight pairs. The results are illustrated in Fig. 2a.

According to the graph, it clearly highlights that both sector capacity and merging conflict violations are decreasing with the increase of the chance constraint probability. For example, there are 18 and 79 capacity and merging conflicts, respectively, when the chance constraint probability is 0.05, while they have reduced to 5 and 15, respectively, when the chance constraint probability is increased to 0.95. Thus, as expected, when the constraints are applied with a higher percentage, the conflicts have reduced in turn decreasing the ATC workload and safety risk of the ATN.

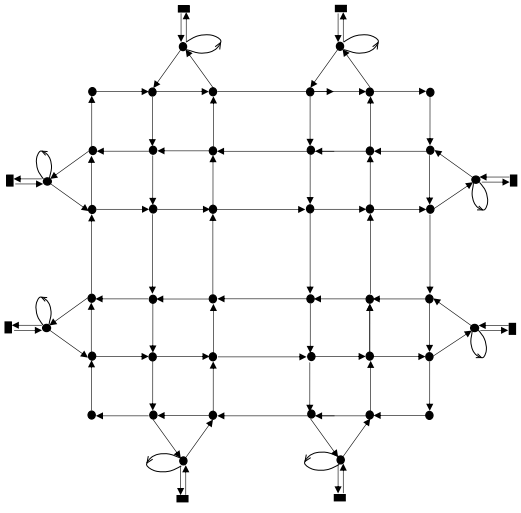

Fig. 1. Simulated grid network - Case Study I

*Average Delay performances with respect to the chance constraint probability:-* The graph in Fig. 2b illustrates the departure, arrival delay profiles, and the number of cancellations with respect to chance constraint probability. According to the results, the average delays have increased when the chance constraints are held with a higher percentage. The reason behind this variation is that flights have to stretch over time to keep the required separations when the constraints are sustained with higher chances. For example, six flights have been canceled when the chance constraint probability is 0.95 since they cannot be scheduled within their bounds. Thus, this induces a trade-off between flight delay and safety in such a way that it enhances the safety of ATN in the expense of flight delays.

### *4.2 Case Study II - ASEAN network*

In this case study, we use three flight information regions (FIRs) of the ASEAN air traffic network, which is composed of Singapore, Kuala Lumpur, and Kota Kinabalu FIRs as shown in Fig. 3. The purpose of this case study is to assess the applicability of the proposed model in a realistic large scale system. The network consists of 275 air routes, 78 waypoints, 25 airports, and 103 origin-destination (OD) pairs. The flight plan data were extracted from the Flightradar24 tool (Flightradar24 (2006)). The same FIR boundaries are considered as the sector boundaries, thus three sectors.

To illustrate the computational feasibility, we tested our model for two different traffic cases with 695 flights and 1390 flights, which are the normal and the double traffic of this region. The results are tabulated in Table 1. In both cases, when solved with the Gurobi solver, without any modification (referred to as '*Optimal*') takes a long time to generate optimal results. Thus, we set a time limit of 30 min for both normal and double traffic cases. The results obtained at these terminated points are not the global optimal yet very close to the optimal. Moreover, the problem is decomposed into a set of independent flows and solved iteratively as depicted in Algorithm I (referred to as '*MIS*'). The normal traffic case with 695 flights, takes only

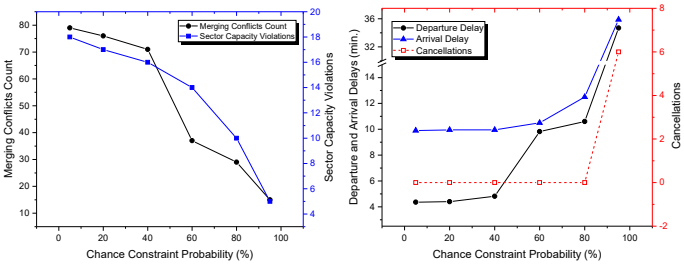


(a) En-route violations

(b) Flight average delay profiles and cancellations

Fig. 2. Performance graphs w.r.t. the chance constraint probability

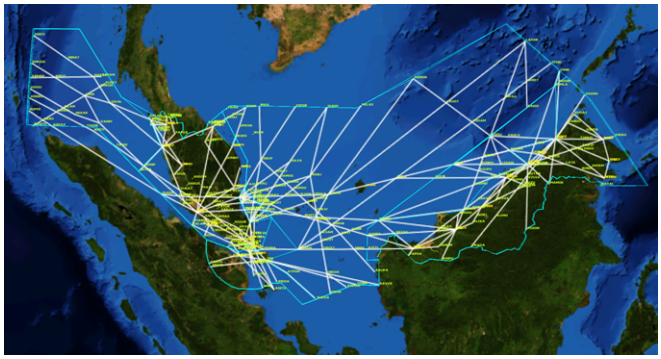

Fig. 3. ASEAN air traffic network - Case Study II

Table 1. CS II - Normal and double traffic results

| Parameters | 695 flights | | 1390 flights | |
|---|---|---|---|---|
| | *Optimal* | *MIS*$^\star$ | *Optimal* | *MIS*$^\star$ |
| Solution time | 30min$^\diamond$ | 3.4min | 30min$^\circ$ | 6.9min |
| Optimality gap difference | 1.76% | | 12.0% | |

$^\diamond$ terminated using time limit and the optimality gap was 0.87%, $^\circ$ - terminated using time limit and the optimality gap was 0.39%, $\star$ - without matrix generation time.

3.4 min to solve the problem whereas, the double traffic with 1390 flights takes around 6.9 min. With regards to the quality of the results, the normal traffic case has an optimality gap of 1.76%, while for the double traffic case, it is 12.0% with respect to the results of the *Optimal*.

Although, we doubled the traffic, the solution time did not increase drastically. The reason is that in this flow model, the decision variables do not increase with the increase of traffic like in a flight-by-flight model. In comparison to our previous work, Sandamali et al. (Under review), which uses a flight-by-flight formulation structure and took 39.8 min to solve a problem with 1390 flights, this approach is approximately 5 times faster than. Thus, it clearly emphasizes the scalability of this model and further highlights the applicability in solving large scale problems, while preserving the quality of the results.

## 5. CONCLUSIONS

The proposed ATFM model is a flow-based formulation for flight routing and scheduling under the consideration of different uncertainty situations. With the flow-based structure, it enhances the scalability, while satisfying link capacity, sector capacity, and waypoint capacity constraints via a chance constraint probabilistic approach. Further, it strengthens the safety of the ATN, while reducing controller workload with competitive flight delays. The experiment results highlight the improved performance of the proposed model in terms of safety, conflicts/violations, scaling capability, and real-time applicability. In future, we expect to expand this work further by incorporating detailed flight information to enhance safety while still retaining the scalability.

## REFERENCES

Balakrishnan, H. and Chandran, B.G. (2014). Optimal large-scale air traffic flow management.

Bertsimas, D., Lulli, G., and Odoni, A. (2011). An integer optimization approach to large-scale air traffic flow management. *Oper. Res.*, 59(1), 211–227.

Bertsimas, D. and Patterson, S.S. (1998). The air traffic flow management problem with enroute capacities. *Oper. Res.*, 46(3), 406–422. doi:10.1287/opre.46.3.406.

Cao, Y. and Sun, D. (2011). Link transmission model for air traffic flow management. *Journal of Guidance, Control, and Dynamics*, 34(5), 1342–1351.

Chen, J., Chen, L., and Sun, D. (2017). Air traffic flow management under uncertainty using chance-constrained optimization. *Transportation Research Part B: Methodological*, 102, 124 – 141.

Clarke, J.P., Solak, S., Chang, Y.H., Ren, L., and Vela, A. (2009). Air traffic flow management in the presence of uncertainty. *Europe Air Traffic Management Research and Development Seminar*.

Flightradar24 (2006). URL `www.flightradar24.com`. Accessed: Aug. 31, 2018.

Gurobi (2015). Gurobi Optimizer Reference Manual. Manual. Houston, TX, USA, 2015.

Linhart, J.M. (2008). Algorithm 885: Computing the logarithm of the normal distribution. *ACM Trans. Math. Softw.*, 35(3), 1–10. doi:10.1145/1391989.1391993.

Sandamali, G.G.N., Su, R., Sudheera, K.L.K., and Zhang, Y. (Under review). A safety-aware real-time air traffic flow management model under demand and capacity uncertainties. *IEEE Transactions on Intelligent Transportation Systems*. (Under major review).

Sandamali, G.G.N., Su, R., and Zhang, Y. (2019). Short-term en route air traffic flow management under departure and wind uncertainties with a heuristic and greedy solution approach. In *2019 American Control Conference (ACC)*, 2121–2126.

Sandamali, G.G.N., Su, R., and Zhang, Y. (2020). Flight routing and scheduling under departure and en route speed uncertainty. *IEEE Transactions on Intelligent Transportation Systems*, 21(5), 1915–1928.

Sandamali, G.G.N., Su, R., Zhang, Y., and Li, Q. (2017). Flight routing and scheduling with departure uncertainties in air traffic flow management. In *2017 13th IEEE International Conference on Control Automation (ICCA)*, 301–306.

Smith, S. and Gilbo, E. (2005). Analysis of uncertainty in ETMS aggregate demand predictions. Volpe National Transportation Systems Center, VNTSC-ATMS-05-05.

Sudheera, K.L.K., Ma, M., and Chong, P. (2019). Link stability based optimized routing framework for software defined vehicular networks. *IEEE Transactions on Vehicular Technology*, 68(3), 2934–2945.

Sun, D. and Bayen, A.M. (2008). Multicommodity eulerian-lagrangian large-capacity cell transmission model for en route traffic. *Journal of Guidance, Control, and Dynamics*, 31(3), 616–628. doi:10.2514/1.31717.

Wei, P., Cao, Y., and Sun, D. (2013). Total unimodularity and decomposition method for large-scale air traffic cell transmission model. *Transportation Research Part B: Methodological*, 53, 1 – 16.

Zhang, Y., Su, R., Sandamali, G.G.N., Zhang, Y., Cassandras, C.G., and Xie, L. (2018). A hierarchical heuristic approach for solving air traffic scheduling and routing problem with a novel air traffic model. *IEEE Transactions on Intelligent Transportation Systems*, 1–14.